Thermosensitive Dielectric Properties in Polyamide–Phenol Hybrid Compounds and Their Application to the Temperature-Sensing Wire

YOSHIO KISHIMOTO, *Heater Equipment Division, Matsushita Housing Products Co., Ltd., Yamatokoriyama, Nara 639-11, Japan,* and TOMIHARU HOSAKA and WATARU SHIMOTSUMA, *Central Research Laboratory, Matsushita Electric Industrial Co., Ltd., Moriguchi, Osaka 570, Japan*

Synopsis

Thermosensitive dielectric properties in polyamide–phenol hybrid compounds have been studied. The polyamide–phenol hybrid compounds are constituted of p-hydroxybenzoate–formaldehyde condensation oligomer dispersed molecularly in nylon 12 and polyamide copolymer. These materials are less hygroscopic than nylon 12 which is the least hygroscopic among polyamide homopolymers. It will be because the phenol group coordinates to amide group as the less hygroscopic "pseudo-water" instead of water. One of these materials has also shown an intrinsic hydrophobic effect of hydrogen bond segment due to the "hybrid effect" between polyamide and phenol. The thermosensitive dielectric properties are based on the temperature dependence of intermolecular hydrogen bond behaviors by amide and phenol groups, which have been discussed in relation with the molecular behaviors. The relationship with polarizations constituting dielectric constant and hydrogen bonding molecular segments, and ac hopping conduction behaviors by proton carriers have also been discussed. These materials are applied as a temperature-sensing material in a flexible thermosensing heater wire, which has three functions, that is, thermosensing, heating, and fusing for safe in the case of an abnormal overheat. As the features for a sensing material, these materials show the humidity low-dependence and highly thermal stability, and will be situated as one of the high-performance sensing material useful for the electric warmer such as an electric blanket.

INTRODUCTION

The electrically thermosensitive properties can be utilized for temperature-sensing devices in electronics. The excellent flexibility and moldability of the thermosensitive polymers make possible the fabrication of flexible thermosensing cable devices useful for temperature detection in wide or flexible areas. The electrically thermosensitive properties, that is, the temperature dependence of admittance, conductance or capacitance is used as temperature signals.[1] The conductance is based on an ionic or electronic conductivity; the ionic conductivity greatly varies with time because of an ionic polarization effect by direct current (dc) field, while the admittance based on electronic conductivity or capacitance never varies with time under the dc field and can be utilized as a reliable sensing signal. As the material which changes capacitance as the temperature signal, polyamide compounds have been studied.[1] However, because the polyamide is hygroscopic, it is

not preferable to be applied as the sensing material. In this paper, thermosensitive dielectric properties in polyamide–phenol hybrid compounds, "New plastic thermistor," which show less hygroscopic and reliable characteristics, are described.

The electrical properties of polyamide have been studied in detail by Baird et al.[2-4] and Seanor et al.[5,6] These reports show that the electric properties relate to the hydrogen bond behaviors of amide group, and the dielectric relaxation and conduction are due to proton and/or electron carrier which generate from the self-dissociation and rearrangement of the hydrogen bonded network. Later many studies have described that the conduction carrier is rather proton than electron.[7-9] In this paper, the thermosensitivity in the dielectric properties are discussed in relation with the hydrogen bond behaviors of the polyamide–phenol compounds, and their application to flexible thermosensing heater (TSH) wire is described below.

THERMOSENSITIVE DIELECTRIC PROPERTIES IN POLYAMIDE–PHENOL HYBRID COMPOUNDS

Experimental

Materials. Two kinds of materials consisting of polyamide–phenol hybrid compounds, materials A and B, where prepared. Material A consists of p-hydroxybenzoate–formaldehyde condensation oligomer (called phenol compound below) and antioxidants molecularly dispersed in nylon 12 homopolymer, and material B consists of that dispersed in polymer alloy of nylon 12 and polyamide copolymer. These compounds were pelletized after blending each raw material by extruder, and the pellets were formed into sheets in 1 mm thick by a hot press machine. Ag paint was coated to both sides of the sheet as electrodes for electrical measurements.

Electrical Measurement. Each sample showed ohmic characteristics in the current–voltage plots in the wide range of the ac and dc fields. Impedance at 60 Hz and resistance were measured under the voltage of 50 V by the potential–fall method. Dielectric constant at 60–100 kHz was calculated from capacitance and conductance measured by dielectric loss meter TRS-10C (Ando Electric Co., Ltd.) and digital LCR meter 4274A (Hewlett-Packard Co., Ltd.).

RESULTS AND DISCUSSION

Thermosensitive Dielectric Properties and Molecular Behaviors. The polyamide–phenol hybrid compounds include hydrogen bonds due to amide and phenol group, which show the thermosensitive dielectric properties and also function as conduction carriers. The electrical properties of these materials are approximately represented by an equivalent circuit such as shown in Figure 1, where C_p is the parallel capacitance, C_s is the series capacitance, R_s is the series resistance, and R_p is the parallel resistance. The C_p is ideal capacitance without dielectric relaxation, and R_p is approximately equivalent to the volume resistivity ρ.
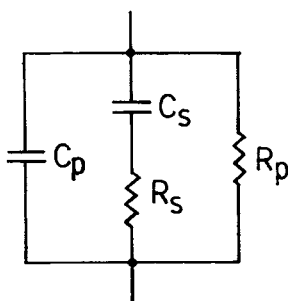
Fig. 1.   Electrical equivalent circuit of the thermosensitive dielectric material.
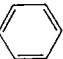
The complex dielectric constant ($\varepsilon^* = \varepsilon' - j\varepsilon''$) consisting of these electrical quantities is represented as follows:

$$\varepsilon' = C_s/[C_0(1 + R_s^2 C_s^2 \omega^2)] + C_p/C_0 \tag{1}$$

$$\varepsilon'' = 1/R_p C_0 \omega + R_s C_s^2 \omega/[C_0(1 + R_s^2 C_s^2 \omega^2)] \tag{2}$$

where ε' is the relative dielectric constant, ε'' is the relative dielectric loss factor, ω is the angular frequency, and C_0 is the capacitance of free space. These dielectric properties can be ascribed to various polarizations such as shown in Table I. The polarizations which contribute to ε' mainly will be ionic, orientation, and atomic polarization due to amide and phenol groups. These polarizations reflect the hydrogen bond behaviors of the amide and phenol groups,[2] and the behaviors give thermosensitivity in dielectric properties as shown in Figure 2. This is understood from the fact that the temperature dependences of impedance for a moisture-absorbed thermosensitive material and a dried one exist in the same temperature range, as shown in Figure 3. This indicates that the polyamide–phenol compound has a thermosensitivity similar to that of the polyamide–water system, and the phenol compound will function as "pseudo-water" in polyamide matrix.

TABLE I
Relationship between the Polarizations and Molecular Behaviors

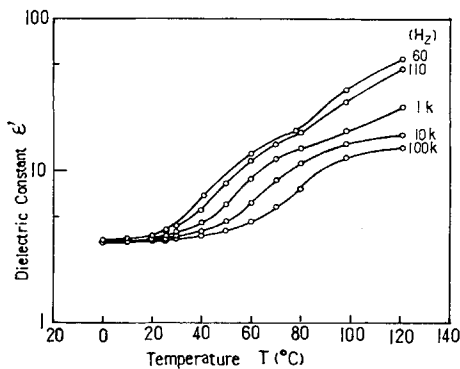| Polarization	Dielectric constant			
	ε'		ε''	
Ionic	Dissociated ions ($H^{\oplus}$, ⬡ —$O^{\ominus}$, —$N^{\ominus}$—CO—)	C_s	Ionic conduction by proton and phenol ion	R_p
Orientation	Polarization by hydrogen bonds of	C_s	Orientation loss of hydrogen bond dipole	R_s
Atomic	Amide group, phenol group, and water	C_p	Negligible	
Electronic	All atoms	C_p	Negligible	

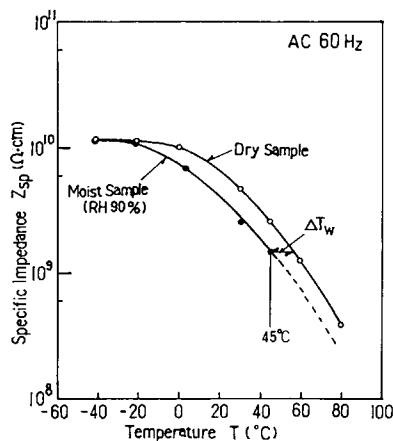Fig. 2. Temperature dependence of dielectric constant of material A.

Fig. 3. Temperature dependence of specific impedance for moisture-absorbed material B and a dried one.

On the other hand, the dielectric loss factor mainly reflects an ionic conductivity due to proton conduction and an orientation loss due to rotational resistance of molecular dipoles. The conduction of polyamide is reported to be due to proton carrier,[7-9] and it will be understood from the constancy of current under dc component field discussed later. The thermosensitive material is composed of polyamide and p-hydroxybenzoate–formaldehyde condensation oligomer, and these are almost immobile bulky molecules under the electric field. In these compounds, proton is the most mobile carrier. The transition of impedance from X_c to R component in Figure 9(b) described later, that is, the transition in Figure 12, corresponds to the transition of proton from a bound ion to a mobile ion, while the orientation loss will be caused by polar segments in the polymer, that is, amide, hydroxyl, and ester groups. These polarizations approximately contributes to C_s, C_p, R_p, and R_s as shown in Table I. The C_p is equal to the capacitance of the equivalent circuit in case of $R_p = \infty$ and $R_s = \infty$, that is, in the case of no conduction carrier. Therefore, the C_p is mainly due to polarization at high frequency where the polarization by the carrier cannot respond, and is approximately equivalent to dielectric constant ε'_∞ at infinite frequency. The C_s and R_s will relate to dielectric relaxation behaviors of hydrogen bond segments.

equivalent to dielectric constant ε'_∞ at infinite frequency. The C_s and R_s will relate to dielectric relaxation behaviors of hydrogen bond segments.

Humidity Dependence. Polyamide is hydrophilic because of the amide group therein, and it is well known that the hydrophilic property is proportional to the concentration of amide group.[10] The water in the polyamide functions as plasticizer of polyamide, and lowers a glass transition temperature. Each material in this study includes the above-mentioned phenol compound, and shows the less-hygroscopic effect and the plasticized one by coordinating to the amide group instead of water molecules. Figure 4 shows the moisture absorption isotherm at 45°C of each material. The polyamide–phenol hybrid compounds show lower dependence on humidity than nylon 12, which is the least hygroscopic among polyamide homopolymer. Because polyamide is hydrophilic, the nylon 12 slightly shows inverse S-letter type curve based on the Sigmoid type absorption.[10] However, the materials A and B show the Freudlich type absorption, i.e., hydrophobic, rather than that. The rate of moisture absorption was measured in sheet samples of 1 mm thick in an oven of 45°C RH 90%. It shows straight lines in $\Delta W - t^{1/2}$ plots, where ΔW is the moisture content and t is the time. The diffusion of moisture is considered to be the Fickian type, and the diffusion coefficients D are determined from the following diffusion equation:

$$D = (q/Q)^2 \times \pi \times (l/2)^2/4t \tag{3}$$

where q is the moisture content, Q is the saturated moisture content, and l is the thickness of sheet sample (1 mm) because of both side diffusion of sheet. The determined values of D (cm^2/s) were 1.3×10^{-8} (nylon 12), 1.3×10^{-8} (material A), 2.5×10^{-8} (material B) and 4.7×10^{-8} (polyamide copolymer). The value of D for material A is equal to that of nylon 12, but material B has a high D value, i.e., a high rate of absorption as well as the polyamide copolymer blended as matrix polymer therein.

The temperature sensing error ΔT_w by humidity, which is defined as temperature deviation from 45°C to the temperature of the dried sample showing the same impedance as that at 45°C of the moisture-absorbed one as shown in Figure 3, depends on the relative humidity, as shown in Figure
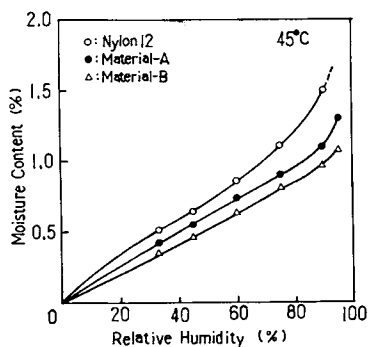

Fig. 4.   Moisture absorption isotherm at 45°C of each material. (○) nylon 12; (●) material A; (△) material B.

5. The value of ΔT_w (°C) of samples moisture-absorbed at RH 90% was 26 in nylon 12, 18 in material A, and 11 in material B, respectively. From Figures 4 and 5, the relationship between ΔT_w and moisture content is represented in Figure 6. Apparent moisture absorption in the material can be improved by fillers such as glass fibers or inorganic powders mixed in polyamide. However, the value of ΔT_w reflects the electrical properties based on the hydrogen bond. For the purpose of the lowering of ΔT_w, the hydrogen bonds themselves must become hydrophobic, different from that of the apparent moisture absorption. Polyamide is generally immiscible with other materials because of the strong intermolecular hydrogen bonds. In these materials A and B, phenol compounds are miscible with nylon 12 by the strong hydrogen bonds, and is molecularly dispersed in polyamide matrix. Figure 6 shows that material A is plotted on the nearly same line as nylon 12. From this fact, it is deduced that the phenol compound functions as less hygroscopic "pseudo-water" instead of water in nylon 12 matrix, and the hydrophobic property of phenol group constituted of binding the hydroxyl group and hydrophobic benzene ring reduces the hygroscopic property of polyamide. On the other hand, material B has a lower ΔT_w than that corresponding to the moisture content. This deviation is a new effect, which is different from both the plots of the polyamide copolymer and material A
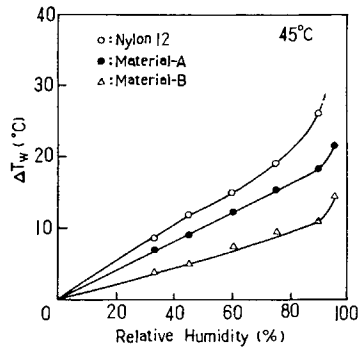

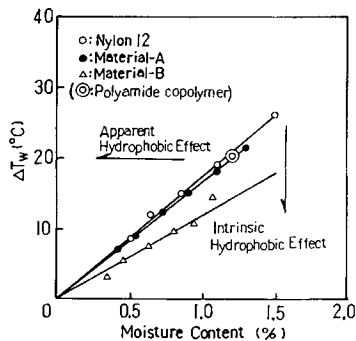Fig. 5.   Humidity dependence of ΔT_w of each material: (○) nylon 12; (●) material A; (△) material B.

Fig. 6.   Relationship between ΔT_w and moisture content for each material: (○) nylon 12; (●) material A; (△) material B, (◎) polyamide copolymer.

shown in the figure. This effect will be understood as the "hybrid effect" between polyamide and phenol for the intrinsic hydrophobic effect in comparison with material A. That is, material B shows very low humidity dependency due to the "hybrid effect," and gives a correct temperature signal in application to the temperature sensor described later. This "hybrid effect" is presumed to be due to the excellent miscibility of the phenol oligomer with the very disordered free volume of the polyamide copolymer.

ac Conduction. ac conductivities are calculated by the following equations[10,11]:

$$\sigma'_{ac} = \omega \varepsilon_0 \varepsilon'' \tag{4}$$

$$\sigma'_{ac}(\omega) = \sigma'_{ac} - \sigma_{dc} \tag{5}$$

where ε_0 is the permittivity of free space and σ_{dc} is the dc conductivity. The frequency dependence of $\sigma'_{ac}(\omega)$ for material A is shown in Figure 7, where the σ_{dc}'s at 98 and 121°C were 1.77×10^{-9} and 1.36×10^{-8} S cm^{-1}, respectively, and σ_{dc} at 26°C was negligibly small. By applying the equation $\sigma'_{ac}(\omega) = A \times \omega^s$ to the figure, the values of s were determined from the slope, where A is the proportional constant and s is the exponent.

On the other hand, the Kramers–Kronig relationship requires that relative dielectric constant varies with frequency as $\varepsilon' = \varepsilon'_\infty + B \times \omega^{s-1}$, where ε'_∞ is the relative dielectric constant at infinite frequency. The value of s determined from the frequency dependence of $\varepsilon' - \varepsilon'_\infty$ are also shown in the figure, where ε'_∞ is the value of ε' at 10^7 Hz determined by extrapolation of ε' in 60–100 kHz range. The figure shows that the value of s determined from $\log \sigma'(\omega) - \log f$ is approximately equal to that from $\log(\varepsilon' - \varepsilon'_\infty) - \log f$. It has been reported that the value of s has relationship with the multiplicity of hopping in electronic conduction,[11,12] and the theory has been

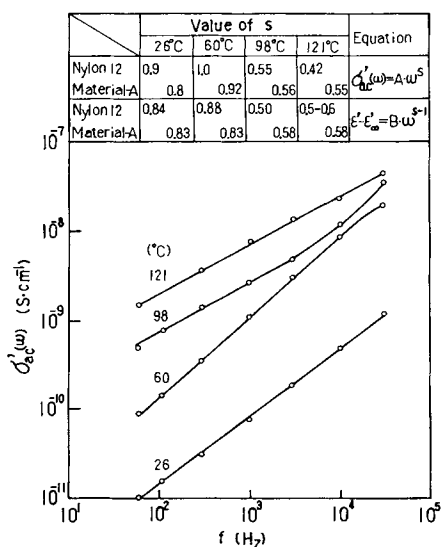|	Value of s				Equation
	26°C	60°C	98°C	121°C	
Nylon 12	0.9	1.0	0.55	0.42	$\sigma'_{ac}(\omega)=A\cdot\omega^s$
Material-A	0.8	0.92	0.56	0.55	
Nylon 12	0.84	0.88	0.50	0.5–0.6	$\varepsilon'-\varepsilon'_\infty=B\cdot\omega^{s-1}$
Material-A	0.83	0.83	0.58	0.58	

Fig. 7.   Frequency dependence of real conductivity $\sigma'_{ac}(\omega)$ for material A.

discussed also in the material of ionic conduction.[13,14] If applying the theory to these materials which will be protonic conduction, Figure 7 shows that the proton hopping varies fron single to multiple with increasing temperature if considered from the decrease of s. The dc conductivity is due to the continuing percolation of carriers between electrodes and will reflect the most probable hops, while ac one reflects all short-range hops which become shorter in terms of the numbers of consecutive hops as the frequency increases, and will represent all possible hops of entire set of transition regardless of whether they can give rise to percolation or not, as shown by Hill and Jonscher.[13] The frequency-dependent $\sigma'_{ac}(\omega)$ and $\varepsilon' - \varepsilon'_\infty$ in ac conduction correspond to $1/R_s$ and C_s of equivalent circuit shown in Figure 1, respectively. The $\sigma'_{ac}(\omega)$ behaviors will reflect the short-range hops of proton carriers in the hydrogen-bonded network, while the $\varepsilon' - \varepsilon'_\infty$ will reflect the ionic or orientation polarization behaviors of hydrogen bond segments in the polyamide–phenol compound. The high values of s at 60°C may reflect the transient molecular behaviors near the glass transition temperature.

APPLICATION TO THE TEMPERATURE-SENSING WIRE

Experimental

The polyamide–phenol hybrid compounds, materials A and B, are applied to thermosensitive dielectric layer in a flexible thermosensing heater (TSH) wire as shown in Figure 8. The thermosensitive dielectric layer was formed in thickness of 0.3 mm by extruding the pellets by means of an extruder for wire production, where a polyester core yarn, copper-alloy wire electrodes, and a plasticized poly(vinyl chloride) insulation jacket were used. Its electrical properties were measured in the similar method as described in the previous section.

RESULTS AND DISCUSSION

Constitution of the Temperature-Sensing System. The TSH wires are cable-formed temperature sensors constituted of materials A and B as shown in Figure 8, and have three functions: temperature sensing, heating, and fusing for safe in the case of abnormal overheat. The heating is performed by outer-wound spiral heating electrode, and the wire has the same wattage per length. The TSH wire needs the temperature characteristics detecting both average temperature and local overheat as shown in Figure 9(a), and
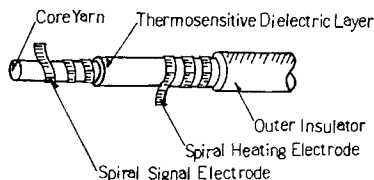

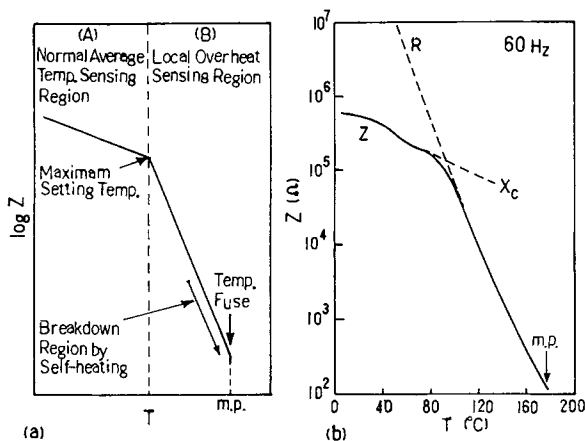Fig. 8.   Structure of flexible thermosensing heater wire.

Fig. 9. Temperature dependence of impedance of flexible thermosensing heater wire.

functions as temperature fuse at a melting point in the case of abnormal overheat. For the purpose of the detection of the average temperature, it is preferable that the TSH wire have a comparatively low temperature coefficient of impedance in order to be controlled in connection with the electronic circuit, and, for the purpose of that of the local overheat, have a very high one at a high temperature region. Because the equivalent circuit of the TSH wire corresponds to the parallel impedance circuit along the direction of its length, the increase of local current by the local overheat preferentially contributes to the temperature signal, and the wire functions to suppress the temperature of the local segment in minimum. Figure 11 shows that the suppression effect is remarkable and the temperature of the local segment is controlled at fairly low temperature. When it is applied to, e.g., an electric blanket, this effect functions to keep the safety from overheat in folded or tacked parts of the blanket. An electronic circuit controlling the TSH wire is constituted as shown in Figure 10, and forms a heating appliance with the high safety. In Figure 10, the temperature signal from the THS wire is detected through a temperature sensing circuit, and, compared with a signal of temperature setting circuit by a control circuit, controls the on–off operation of the thyristor. A positive cycle of the ac field is utilized for heating, while a negative cycle is utilized for sensing the temperature. When the thyristor is on-state, the potential applied to the thermosensitive dielectric layer is full wave of the ac field on one side, and is a half-wave of the ac field on another side connecting the thyristor. Therefore, the material of the thermosensitive layer needs to have constant a sensor impedance even under such a dc-component field. The temperature-fuse operation is performed as follows: A local segment of the thermosensitive dielectric layer melts by an abnormal overheat, two wound-electrodes short-circuit, a resistor set in safety circuit generates heat, and a temperature fuse combined in main circuit melts to cut a source circuit. For the purpose, polyamide, which has a sharp melting point and a high melt-flow index, is the most preferable. Therefore, the polyamide has been selected as the base material in this study.
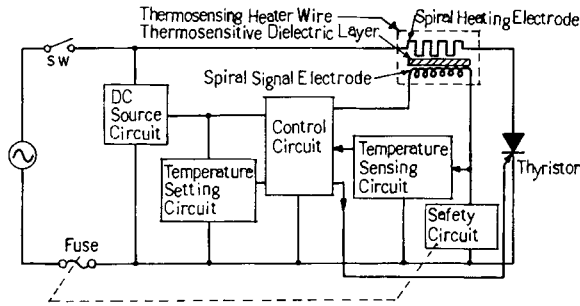
Fig. 10.   Block diagram of temperature control circuit using flexible thermosensing heater wire.
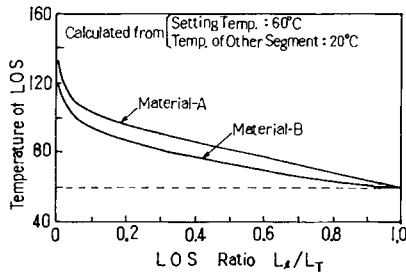

Fig. 11.   Suppression effect of local overheat by the TSH wire composed of materials A and B: (LOS) Local overheat segment; (L_l) LOS length; (L_T) total length.

Impedance Characteristics. The TSH wire shows the ohmic characteristics in the current–voltage plots at the ac or dc field. Figure 9(b) shows the temperature dependence of impedance at 60 Hz for flexible TSH wire. In the temperature range below 90°C, capacitive reactance X_c is predominant, and above that the resistance component R contributes. In the impedance range below 10^3–10^4 Ω (specific impedance of thermosensitive layer: about 10^7 Ω cm), a self-heating by Joule heat occurs, the thermosensitive layer reaches at melting point, and the TSH wire short-circuits. It is desirable that the maximum setting temperature be set below the transition temperature from the X_c to the R component.

The $\log Z_{sp}$–$1/T$ characteristics of each thermosensitive dielectric material, as shown in Figure 12, have two straight lines in the range from room temperature to melting point, where Z_{sp} is specific impedance at 60 Hz and T is absolute temperature. The transition temperature from the X_c to the R component is 87°C in material A and 71°C in material B. The thermistor Bz constants were calculated by the equation $Z_{sp} = Z_0 \times \exp(Bz/T)$. The values of Bz constants for material A are 3800K in the temperature range below 87°C and 13,000K above that. On the other hand, the value for material B are 3800K in the temperature range below 71°C and 11,000K above that. Each Bz constant is a preferable value in that below the transition temperature and has very high values above that so as to minimize the local overheat temperature in the TSH wire. The suppression effect of local overheat by the TSH wire is shown in Figure 11, where the high Bz constant
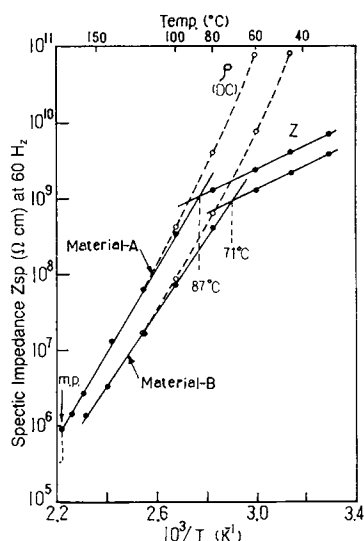
Fig. 12.   Log Z_{sp}–$1/T$ plots of materials A and B.

at high temperature range contributes to suppress markedly the local overheat. An application of high voltage to low impedance thermistor causes a thermistor breakdown by a self-heating, and it functions as well as a temperature fuse in the case of abnormal overheat. Therefore, the material A with high impedance is suitable for an application of a high voltage, e.g., ac 220 V and the material B is suitable for the low voltage of ac 100–120 V.

Reliability. The reliability of temperature sensor is due to stabilities of the temperature signal, i.e., the stabilities in thermal, humid, or electrical environments. For the purpose of the accurate temperature sensing, it is necessary that the sensing material has not only the thermal stability, but has the humid and the electrical ones. For the thermal stability, it is necessary that the sensing material itself is not only stable, but metal electrodes in contact with it also keep its surface clear always. Therefore, the thermosensitivve material has been prepared from the reductive components, i.e., a phenol compound, formaldehyde, and antioxidants which will function as reductants. When the TSH wire is combined with electronic circuit such as shown in Figure 10, the maximum dc-component field applied to the thermosensitive dielectric layer is a half-wave field of ac in the side connecting a thyristor when it is on-state. The application of this dc field often causes an impedance change with time in ordinary polymeric materials by the ionic polarization effects. However, the TSH wires constituted of material A or B show stable characteristics even in an accelerating examination at high temperature as shown in Figure 13. The electric field strength of the dc component to the thermosensitive dielectric layer is a very high field of 2300 V/cm. In spite of it, the wire has surprisingly stable characteristics. In this figure, $(I_{60})_0$ is current at 60°C before examination and nearly corresponds to maximum setting temperature for appliances. I_{120} is the current at 120°C in sample passing test times, and the value of $I_{120}/(I_{60})_0$ approximately represents the measure of the suppression effect of local overheat
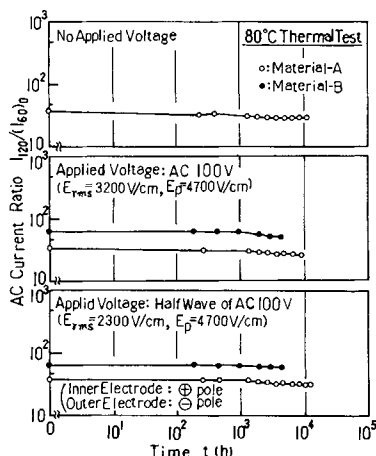
Fig. 13. Thermal stability at 80°C of electrical characteristics for the TSH wire. (Electrical field strength of thermosensitive dielectric layer: E_{rms} is the effective value and E_p is peak value.)

temperature. Figure 13 shows that the suppression effect is high and is also kept throughout long times. This excellent dc-field endurance is due to the fact that the dc-component field is applied so that the bulky phenol anion constituted of p-hydroxybenzoate–formaldehyde condensation oligomer in the layer migrates toward the inner side of its cylindrical cross section, which is a closed structure. That is, owing to the fact that the polarity of the dc field is positive on the inner side, the bulky phenol-anions are hardly able to migrate toward the closed inner side even under such a high dc-component field and the composition of the layer material is kept nearly constant. The $I_{120}/(I_{60})_0$ of material B is higher than that of material A, and the material B is estimated to depress the local overheat temperature lower by about 15°C than material A from Figure 12. In an accelerating test at 100°C, these materials have long life times of 3000–6000 h, and ultimately show very low impedances due to the drop of molecular weight so as to keep final safety, i.e., give a low temperature signal so as to turn off the thyristor. The material B will be evaluated to be one of the best sensing materials showing optimum temperature characteristics. The characteristics of materials A and B are summarized as shown in Table II. Here, the TSH wires show a little lower Bz constants than those of the materials owing to the loose contact of wound wire electrodes to the cylindrical thermosensitive layer.

Thus, thermosensitive dielectric material consisting of the polyamide–phenol hybrid compounds, i.e., materials A and B constitute the high-performance temperature sensor, and can be utilized as a cable-formed device having three functions described above. Moreover, the materials can be formed in sheets and tapes, and can detect temperatures in flexible or wide area. These devices are expected to be applied not only to electric warmers such as an electric blanket, a carpet and a rug, but also extensively to security systems such as a fire-alarm apparatus and a leak oil-alarm one, or air conditioners.

TABLE II
Characteristics of Flexible Thermosensitive Dielectric Materials

Item	Material A	Material B	Remark
Electrical properties			
Specific impedance at 60°C			
(Ω cm)	2×10^9	1.3×10^9	
Thermistor 30–60°C (K)	3800	3800	at 60 Hz
Bz constant 60–120°C (K)	8000	10000	
Mechanical properties			
Tensile strength (kg/cm^2)	490	450	
Elongation (%)	290	300	ASTM D 638
Bending modulus (kg/cm^2)	6800	3000	ASTM D 790
Molding temperature (°C)	190–240	180–220	
Melting point (°C)	176	174	
Water absorption (%)	1.1	0.95	45°C 90% RH
Weight loss (%)	2.1	1.6	120°C 300 h
Electrical Properties of thermosensing heater wire (20 m length)			
Impedance at 60°C (kΩ)	250	170	
Thermistor 30–60°C (K)	2700	2800	at 60 Hz
Bz constant 60–120°C (K)	7000	9000	

References

1. W. Shimotsuma and Y. Kishimoto, *Densizairyo*, **13**(11), 83 (1974).
2. R. J. Meakins and R. A. Sack, *Austr. J. Sci. Res.*, **A5**, 135 (1952).
3. M. E. Baird, *J. Polym. Sci., Part A-2*, **8**, 739 (1970).
4. M. E. Baird, G. T. Goldsworthy, and C. J. Creasey, *Polymer*, **12**(13), 159 (1971).
5. D. A. Seanor, *J. Polym. Sci., Part A-2*, **6**, 463 (1968).
6. D. A. Seanor, *J. Polym. Sci., Part C*, **17**, 195 (1967).
7. S. Nakamura, G. Sawa, and M. Ieda, *Jpn. J. Appl. Phys.*, **18**(5), 995 (1979).
8. Bui Ai, Hoang The Giam, R. Loussier, and P. Destreul, *J. Non-Cryst. Solid*, **23**, 299 (1977).
9. S. Hirota, *J. Appl. Phys.*, **50**(5), 3007 (1979).
10. Soc. Polym. Sci., Jpn. Ed., *High Polymer and Water* (in Japanese), Saiwai Shobou, Tokyo, 1972, p. 9.
11. N. F. Mott and E. A. Davis, *Electronic Process in Non-Crystalline Materials*, Clarendon, London, 1971.
12. K. Saha, S. C. Abbi, and H. A. Pohl, *J. Non-Cryst. Solid*, **22**, 291 (1976).
13. R. M. Hill and A. K. Jonscher, *J. Non-Cryst. Solid*, **32**, 53 (1979).
14. H. Shimokawa, A. Ohashi, and M. Ueda, *J. Phys. D: Appl. Phys.*, **13**, 107 (1980).